analytical chemistry

Article

pubs.acs.org/ac

Constant Flow-Driven Microfluidic Oscillator for Different Duty Cycles

Sung-Jin Kim,[†] Ryuji Yokokawa,[†,‡] Sasha Cai Lesher-Perez,[†] and Shuichi Takayama*[,†,§,⊥]

[†]Department of Biomedical Engineering, University of Michigan, Ann Arbor, Michigan 48109, United States

[‡]Department of Microengineering, Kyoto University, Yoshida-honmachi, Sakyo, Kyoto, 606-8501 Japan

[§]Department of Macromolecular Science and Engineering, University of Michigan, Ann Arbor, Michigan 48109, United States

[⊥]Division of Nano-Bio and Chemical Engineering WCU Project, UNIST, Ulsan, Republic of Korea

Supporting Information

ABSTRACT: This paper presents microfluidic devices that autonomously convert two constant flow inputs into an alternating oscillatory flow output. We accomplish this hardware embedded self-control programming using normally closed membrane valves that have an inlet, an outlet, and a membrane-pressurization chamber connected to a third terminal. Adjustment of threshold opening pressures in these 3-terminal flow switching valves enabled adjustment of oscillation periods to between 57 and 360 s with duty cycles of 0.2−0.5. These values are in relatively good agreement with theoretical values, providing the way for rational design of an even wider range of different waveform oscillations. We also demonstrate the ability to use these oscillators to perform temporally patterned delivery of chemicals to living cells. The device only needs a syringe pump, thus removing the use of complex, expensive external actuators. These tunable waveform microfluidic oscillators are envisioned to facilitate cell-based studies that require temporal stimulation.

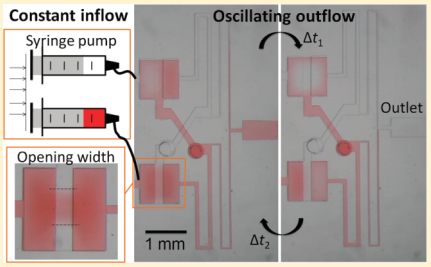

Cells exist in highly dynamic environments consistently being exposed to biochemical and physical stimulation.[1−3] A wide range of microfluidic devices have been proposed to recreate these dynamic environments to more accurately capture cell behavior.[4] Although previous systems aiming to periodically stimulate cells have functioned successfully,[5−11] these systems require external equipment, such as expensive electronic control units in conjunction with microfluidic devices. To minimize the amount of external equipment, recent studies have focused on the development of microfluidic devices that use networks of monolithic, microfluidic valves.[12]

Among microfluidic valves,[12−21] normally closed (NC) membrane valves[13−18] are of particular interest because the NC membrane valve is analogous to a p-channel enhanced mode MOSFET (pMOS, see Figure 1A).[18] With a transistor like the pMOS, an electronic circuit can realize embedded functions and thus eliminates the need of external control. Through the analogy of electronic circuits, NC 3-terminal (source, drain, and gate terminal) pneumatic valves are successfully applied to pneumatic microfluidic logic circuits, thereby greatly eliminating the number of external equipment.[16,17] Owing to the 3-terminal structure of the NC pneumatic valves, which is structurally more analogous to pMOS, structural analogy of the electronic circuit is more easily applied. Hydraulic microfluidic systems that can be applied to cell studies, however, have used NC 4-terminal or 2-terminal valves (i.e., gate has an inlet and outlet, or there is no gate), thus making the architecture of the hydraulic circuit different from that of the electronic circuit.[13−15] With the NC 4-terminal hydraulic valves and only one syringe pump that provides two constant inflows, we have recently implemented the periodic oscillation of outflows.[15] Although the system is useful because of the analogous function of DC to AC conversion, the 4-terminal valve-design is limited in its structural analogy of electronic circuits. As a result, the system has potential limitations to directly expand to more useful functions analogous to electronic circuits. A more immediate drawback of the previously reported microfluidic oscillator is its inherent duty cycle of 0.5. In other words, a different duration time of each outflow is difficult to obtain unless more external equipment (e.g., two syringe pumps with different flow rates) is used. Duty cycle adjustability, however, is indispensible for cell studies[8,22−24] and needs to also be achieved with minimal external equipment.

Here, we describe constant flow-driven oscillators that achieve different duty cycles using NC 3-terminal valves. With a single syringe pump that can accommodate two syringes (Figure 1B), we achieve oscillation of two outflows having different duty cycles. First, we show that NC 3-terminal valves, rather than 4-terminal ones, can realize microfluidic oscillators. We then present control of the threshold pressure by regulating the opening width of the valve (w_o, Figure 1C) and its effects on duty cycle. Finally, we present periodic cell staining to demonstrate the suitability of our device for temporal stimulation of cells.

Received: October 30, 2011
Accepted: December 8, 2011
Published: December 29, 2011

   dx.doi.org/10.1021/ac202866b | *Anal. Chem.* 2012, 84, 1152−1156

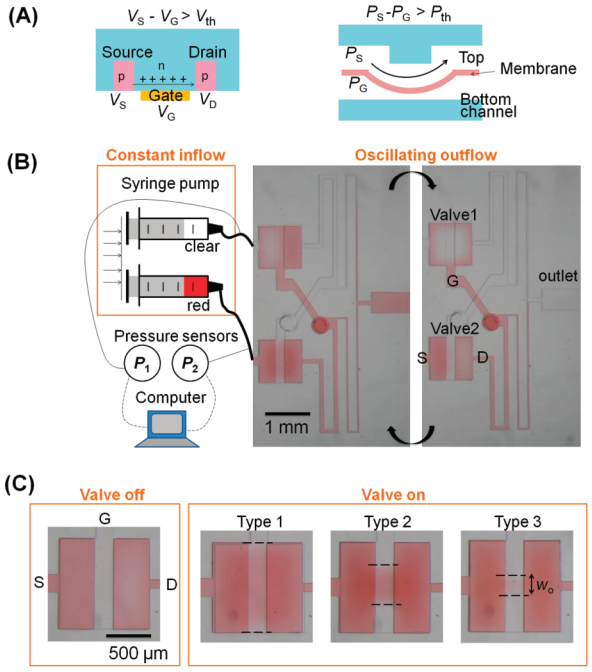

Figure 1. Constant flow-driven microfluidic oscillator. (A) p-type enhanced mode metal oxide field effect transistor (pMOS) and its functional similarity to a normally closed 3-terminal valve. In pMOS, V_S and V_G are the voltages at the source and gate, respectively, and V_{th} is a threshold voltage. Similarly, in the normally closed valve, P_S and P_G are the source and gate pressures, respectively, and P_{th} is a threshold pressure to open the valve. Analogous to pMOS, valve is on (open) only when $P_S - P_G > P_{th}$. (B) Experimental setup and micrograph of the oscillator. S, G, and D are source, gate, and drain terminals, respectively. (C) Valve off and on states. To control P_{th}, the opening width (w_o, see dotted lines) of the valve is changed. w_o of type 1, 2, and 3 valves are 1000, 460, and 200 μm, respectively. Three representative devices are used for the experiment: a type 1 valve is always used as valve 1, whereas different valves are used as valve 2 in each device. Device 1 has type 1 and 1 valves, device 2 has type 1 and 2 valves, and device 3 has type 1 and 3 valves.

MATERIALS AND METHODS

Device Fabrication. Microfluidic device fabrication was performed using soft lithography.[25] A master mold was fabricated by a deep reactive ion etching of a Si wafer. We used direct etching of Si on the mold rather than photolithography of SU-8 on the wafer, because the adhesion of SU-8 was poor for long, 40 μm-wide narrow channels. The master mold was silanized with tridecafluoro-1,1,2,2-tetrahydrooctyl-1-trichlorosilane (United Chemical Technologies, PA, USA) in a desiccator for 12 h to promote facile demolding of casting material. The casting material was made from poly(dimethylsiloxane) (PDMS) prepolymer and curing agent (Sylgard 184, Dow Corning, MI, USA) at a 10:1 ratio and was used for the device. The device was composed of three layers: the top and the bottom layers, which contained the microfluidic channels, were cast against the master mold. They were then cured in a 120 °C oven for 2 h. The middle layer is a membrane layer (40 μm-thickness for device characterization and 20 μm-thickness for cell experiment) and was spin-coated on a silanized glass slide and then cured in the oven for 20 min. The PDMS stamps[15,26] were made using a similar method to the fabrication of the top and bottom layers, except stamps were only cured in the oven for 5 min.

For the bonding of the three layers (see Figure S1 of Supporting Information), we used a plasma oxidizer (Model PDC-001, Harrick Plasma, NY, USA) with air for 2 min. First, the middle layer, while still on the glass slide, was bonded to the bottom layer after plasma treatment of the two layers and cured in the oven for 5 min. After peeling off the bonded two layers from the glass slide, we punched connection holes using a 350 μm biopsy punch in the middle layer. In the top layer, inlet and outlet holes were punched, and the top layer was aligned and bonded with the other bonded two layers followed by the plasma treatment. To ensure w_o (Figure 1C) of the valve, we placed[15] PDMS stamps on the middle layer of the valve area during plasma treatment and stamped[26] the top layer of the valve after plasma treatment. Device 1, 2, and 3 have type 1 and 1, type 1 and 2, and type 1 and 3 valves (Figure 1C), respectively.

Experimental Setup. Pressure sensors were connected at the inlets to measure source pressures (P_S, Figure 1A). Different pairs of pressure sensors were used for the devices, because the devices had different pressure ranges. A pair of two pressure sensors (Model 142PC05G, Honeywell, NJ, USA) was used for device 1 and 2, and another pair (Model PX139-015D4V, Omega Eng., CT, USA) was used for device 3. The fluidic capacitances of the first and the second pair of the sensor systems including connection tubes were measured in average as 5.3×10^{-13} and 6.3×10^{-13} m^5/N, respectively. Pressure data were obtained at a 50 ms sampling rate and saved on a computer. Using commercial software (Origin, OriginLab, MA, USA), we filtered out the noise signal of the pressure data from device 3 with a low pass filter at a cut off frequency of 1 Hz. A syringe pump (Model Fusion 400, Chemyx, TX, USA) was used to provide a constant flow, and the devices were monitored using a stereo microscope (Model SMZ 800, Nikon, Japan) and a digital camera. Working solutions were deionized water with/without a red food dye. To facilitate the introduction of working solutions, the device was put in a vacuum for 5 min. We used commercial software (PLECS, Plexim GmbH, Switzerland) to develop the theoretical model of the oscillator.

Cell Culture, Seeding, and Imaging. C2C12 cells were cultured in Dulbecco's Modified Eagle's Medium (DMEM) (Invitrogen) under 37 °C, 5% CO_2 on a plastic tissue culture dish.[27] Then, 0.25% Trypsin/EDTA (Gibco) was used to detach cells from the dish. For the cell seeding in the microchannel outlet (Figure 1B), fibronectin (50 μg/mL in PBS) was injected along the microchannel and incubated at room temperature for 10 min to coat the channel surface. Then, cells were injected into the microchannel and maintained with DMEM under 37 °C, 5% CO_2 for a day. For the periodic staining of cells, 1 μM fluorescent dye (SYTO 84, Invitrogen) was used in TE buffer, and cells were imaged with a TE2000-U Nikon inverted microscope and a CoolSnap HQ2 camera (Photometrics, Tucson, AZ). The excitation and emission filter wheels were controlled by the Lambda 10-3 Shutter Controller (Sutter Instruments, Novato, CA). Images were acquired every 5 s, and an exposure time of 1 s was used. The program MetaFluor (Molecular Devices, Downington, PA) was used for image acquisition and processing; for each image, the background was subtracted.

RESULTS AND DISCUSSION

Function of NC 3-Terminal Valve for Oscillation. The microfluidic oscillator with NC 3-terminal valves has a different

dx.doi.org/10.1021/ac202866b | Anal. Chem. 2012, 84, 1152–1156

arrangement of channels as compared to the previous 4-terminal oscillator.[15] For example, the drain terminal of valve 2 is connected to the gate terminal of valve 1 via a connection channel (Figure 1B,C). Red fluid moves from valve 2's source through its drain terminal to the outlet; however, the fluid does not pass through the gate terminal of valve 1. As a result, without red fluid passing through the gate terminal of valve 1 to the outlet, as it did in previous 4-terminal hydraulic valves, gate pressure of valve 1 is controlled by the source pressure of valve 2.

In the case of valve 2 being off, there is no flow through the drain terminal of valve 2 (Figure 1B). This results in the drain pressure of valve 2 to be 0 and, in turn, makes the gate pressure of valve 1 (P_{G1}) 0. When valve 2 is on, P_{G1} becomes positive. At this moment, because P_{G1} is greater than the source pressure of valve 1 (P_{S1}) due to the inherent fluidic resistance of the downstream channel (Figure S2 of Supporting Information), valve 1 shuts off. (See red region of Figure 2A.) This change results in P_{S1} building up due to the constant red inflow, leading to valve 1 switching on again once $P_{S1} - P_{G1} > P_{th1}$ where P_{th1} is a threshold pressure of valve 1. Because the operating condition also applies to valve 2, constant inflow into the system and the interaction between the two valves through P_S and P_G drive continuous oscillation of the device's outflow.

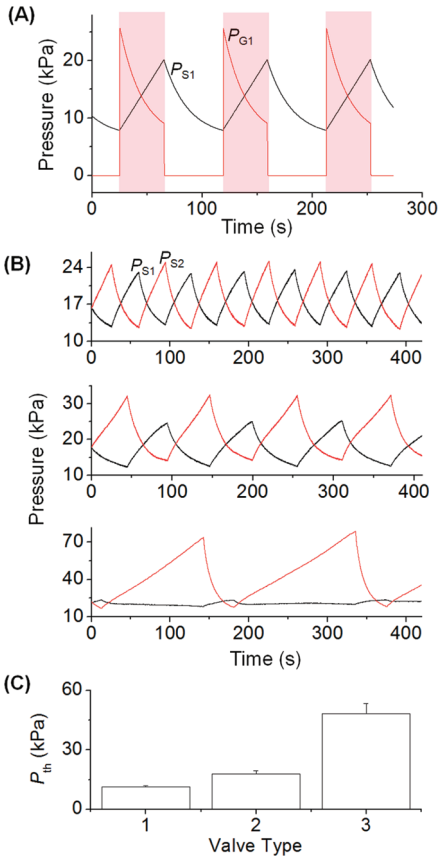

Figure 2. Pressure profiles in the valves. The inflow rate is 10 μL/min in (A) and (B). (A) Theoretical pressure profiles at valve 1 (Figure 1B) of device 2. Red region is valve-off state. (B) Measured pressure profiles. Top, middle, and bottom panels are devices 1, 2, and 3, respectively. Note that the pressure difference between maximum P_{s1} and P_{s2} increases as the asymmetry of w_o increases between the two valves. (e.g., Device 3 has the highest asymmetry in the w_o of the valve; see Figure 1C.) (C) Measured threshold pressure in each valve type.

Effect of Threshold Pressure on Duty Cycle. We used three types of valves with different w_o (Figure 1C) for the oscillators. As w_o becomes narrower, it makes the membrane stiffer near the opening area of the valve. In other words, narrower w_o requires higher pressure to open the valve (i.e., higher P_{th}). As depicted in Figure 2A, P_{S1} (or P_{S2}) builds up when valve 1 (or valve 2) is turned off by P_{G1} (or P_{G2}). In device 1, both valves are symmetric type 1 valves, thus making the time for the accumulation of pressure (valve-off time) the same in the two valves. Consequently, periodic duration time of valve-off is approximately the same within the device (top panel of Figure 2B). In device 1, the slight difference of maximum P_{s1} and P_{s2} comes from size variation and alignment error of stamps. In contrast, devices 2 and 3 contain an asymmetric pair of two valves in each device. Specifically, type 1 and 2 valves are used in device 2, and type 1 and 3 valves are used in device 3. This makes the necessary time for the accumulation of pressure (valve-off time) uneven in each device (middle and bottom panel of Figure 2C). Note that device 3 has the greatest asymmetry in two source pressure profiles due to the highest asymmetry of threshold pressure.

Figure 2C summarizes the threshold pressure (P_{th}) in each valve type, which was measured from Figure 2B and other inflow rate conditions ranging from 2 to 10 μL/min. Although P_{th} is defined as the difference of P_S and P_G at the moment of valve opening, it can be approximated as the difference of P_{S1} and P_{S2} at the moment of valve opening (Figure S3 of Supporting Information) because downstream fluidic resistor is 1 order of magnitude higher than the connection resistor. As we expected, P_{th} of type 3 valve was the highest compared to the other two valve types.

Effects of inflow rate and threshold pressure on oscillation period and duty cycle are illustrated in Figure 3. It should be noted that the range of periods (70−360 s) and duty cycles (0.2−0.5) presented in our study are suitable for cell signaling studies, especially for calcium signaling pathways.[23,24,28] As

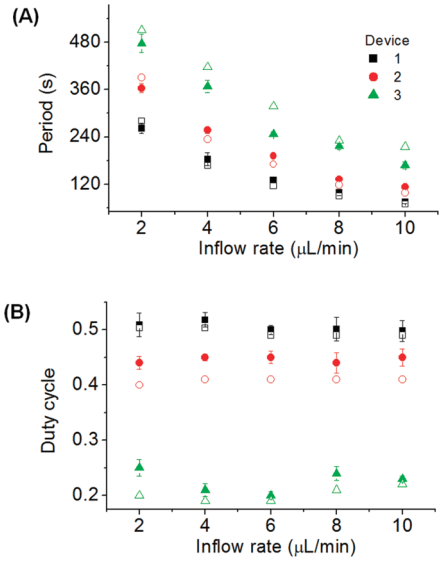

Figure 3. Performance of the constant flow-driven oscillators. Filled and unfilled points are the experimental and theoretical results, respectively, and the error bars were obtained from repeated measurements (n > 8) with a single device type. (A) Oscillation period. (B) Duty cycle.

dx.doi.org/10.1021/ac202866b | Anal. Chem. 2012, 84, 1152−1156

inflow rate increases, oscillation period decreases (Figure 3A). In the off-valve, source pressure characteristic is approximated as $P_S = (Q_{in}/C)t + P_0$ which comes from $Q_{in} = C\ dP_S/dt$, and Q_{in}, C, and P_0 are inflow rate, fluidic capacitance, and initial pressure at time $t = 0$, respectively. Accordingly, P_S builds up faster as Q_{in} increases; this reduces the valve's off-time and, consequently, oscillation period. Also, at the same inflow rate, oscillation period decreases as valve 2 has lower P_{th} (i.e., device 3 to 1). Although off-time of valve 1 is the same in the three devices, lower P_{th} in valve 2 results in shorter off-time for valve 2, thus reducing oscillation period. Figure 3B shows that the duty cycle in reference to the red outflow is controlled from 0.2 to 0.5, correlating to a duration ratio of red to clear ranging from 1:4 to 1:1. Notably, duty cycle remains almost constant in each device, even as the flow rate changes. It is because duty cycle is determined by the off-time ratio between the two valves and the off-time ratio is determined by the ratio of two threshold pressures (Supporting Information). Thus, this device design supplies a constant duty cycle regardless of inflow rate change.

Periodic Cell Staining. To demonstrate that our device is suitable for temporal stimulation of cells,[7−11] we seeded C2C12 cells in the outlet channel (Figure 1B) and performed periodic staining of cells. The fluorescent dye we used is cell-permeable through plasma cell membrane, has a high affinity to nucleic acids, and increases fluorescence upon binding.[29] For the periodic staining of the cell nucleus, we used blank TE buffer and fluorescent solutions. Oscillation of fluorescent intensity matches with that of the two solutions (Figure 4A−C). When the fluorescent solution flowed through valve 1 to the outlet channel, fluorescent intensity at the cell nucleus increased and then saturated (Figure 4D). In contrast, during the duration of blank solution through valve 2, the intensity decreased. In a control experiment, we performed a static cell staining in a Petri dish and observed the fast decrease of fluorescent intensity of stained cell nuclei due to fast photobleaching (Figure S4 of Supporting Information). Unlike the static condition, our device can periodically supply the fluorescent dye. Accordingly, at the on state of valve 1 the fluorescent intensity becomes saturated by the continuous supply of the dye whereas at the on state of valve 2 the intensity decreased by photobleaching and dye dissociation.

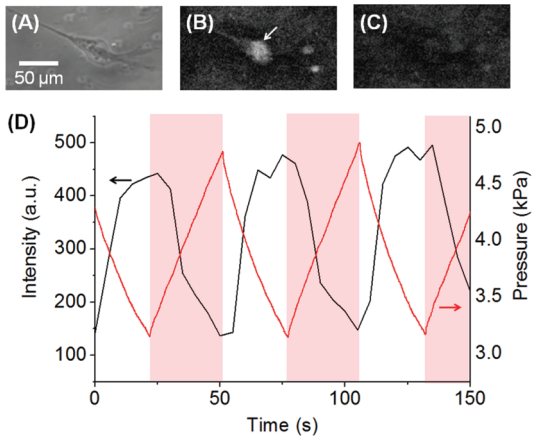

Figure 4. Periodic staining of cell nucleus. (A−C) Micrograph of C2C12 cells in the outlet microchanel (Figure 1B). Nuclei of cells are periodically stained with a fluorescent dye. Phase contrast image is in (A), and images having maximum and minimum fluorescent intensity are shown in (B) and (C), respectively. (D) Fluorescent intensity profile of a cell nucleus (see arrow in (B)) and the corresponding pressure profile at the source terminal of valve 1. Red region is valve-off state for the fluorescent solution, and clear solution flows during this time.

The oscillation period was 57 s with a duty cycle of 0.5 at an inflow rate of 4 μL/min. We used type 1 valves for the two valves (Figure 1), but the membrane was thinner compared to the devices in Figure 3 (20 vs 40 μm). Because thinner membrane results in a lower threshold pressure (2.2 kPa), it takes a shorter time for pressure accumulation (valve-off time). As a result, the oscillation period is faster than that in Figure 3A.

CONCLUSIONS

Our results demonstrate the capability to regulate duty cycles by appropriate design of valves in a self-oscillating microfluidic device. This embedded control of duty cycle enables different duty cycles to be achieved using one syringe pump. By controlling the threshold pressure of normally closed valves, we could implement oscillation periods ranging between 57 and 360 s and a duty cycle ranging between 0.2 and 0.5 at an inflow rate range of 2−10 μL/min. In addition, these devices represent the first examples of realizing oscillatory outflows using normally closed 3-terminal valves that are analogous to p-type MOSFET. Finally, we demonstrate periodic cell staining, thus showing the suitability of these device for live cell studies. These devices are simple, inexpensive tools envisioned to be useful for creating dynamic biochemical and biophysical microenvironments to study cells.

ASSOCIATED CONTENT

Supporting Information

Device fabrication details; theoretical model of the constant flow-driven oscillator; approximation of duty cycle; comparison of staining between static and pulsed; movie of the microfluidic oscillator. This material is available free of charge via the Internet at http://pubs.acs.org.

AUTHOR INFORMATION

Corresponding Author

*E-mail: takayama@umich.edu.

ACKNOWLEDGMENTS

This work was supported by the NIH (GM096040-01 and HL084370-05).

REFERENCES

(1) Brabant, G.; Prank, K.; Schofl, C. *Trends Endocrinol. Metab.* **1992**, *3*, 183−190.
(2) Laurent, G. *Nat. Rev. Neurosci.* **2002**, *3*, 884−895.
(3) Chiu, J.-J.; Chien, S. *Physiol. Rev.* **2011**, *91*, 327−387.
(4) Jovic, A.; Howell, B.; Takayama, S. *Microfluid. Nanofluid.* **2009**, *81*, 3714−3722.
(5) Giridharan, G. A.; Nguyen, M.-D.; Estrada, R.; Parichehreh, V.; Hamid, T.; Ismahil, M. A.; Prabhu, S. D.; Sethu, P. *Anal. Chem.* **2010**, *82*, 7581−7587.
(6) Ogilvie, I. R. G.; Sieben, V. J.; Mowlem, M. C.; Morgan, H. *Anal. Chem.* **2011**, *83*, 4814−4821.
(7) Hersen, P; McClean, M. N.; Mahadevan, L.; Ramanathan, S. *Proc. Natl. Acad. Sci. U.S.A.* **2008**, *105*, 7165−7170.
(8) Bennett, M. R.; Pang, W. L.; Ostroff, N. A.; Baumgartner, B. L.; Nayak, S.; Tsimring, L. S.; Hasty, J. *Nature* **2008**, *454*, 1119−1122.
(9) Kuczenski, B.; Ruder, W. R.; Messner, W. C.; LeDuc, P. R. *PLoS ONE* **2009**, *4*, e4847.

(10) Kim, Y.; Joshi, S. D.; Messner, W. C.; LeDuc, P. R.; Davidson, L. A. *PLoS ONE* **2011**, *6*, e14624.
(11) Kim, Y.; Kuczenski, B.; LeDuc, P. R.; Messner, W. C. *Lab Chip* **2009**, *9*, 2603−2609.
(12) Mosadegh, B.; Bersano-Begey, T.; Park, J. Y.; Burns, M. A.; Takayama, S. *Lab Chip* **2011**, *11*, 2813−2818.
(13) Mosadegh, B.; Agarwal, M.; Tavana, H.; Bersano-Begey, T.; Torisawa, Y.-S.; Morell, M.; Wyatt, M. J.; O'Shea, K. S.; Barald, K. F.; Takayama, S. *Lab Chip* **2010**, *10*, 2959−2964.
(14) Leslie, D. C.; Easley, C. J.; Seker, E. J.; Karlinsey, M.; Utz, M.; Begley, M. R.; Landers, J. P. *Nat. Phys.* **2009**, *5*, 231−235.
(15) Mosadegh, B.; Kuo, C.-H.; Tung, Y.-C.; Torisawa, Y.; Bersano-Begey, T.; Tavana, H.; Takayama, S. *Nat. Phys.* **2010**, *6*, 433−437.
(16) Rhee, M.; Burns, M. A. *Lab Chip* **2009**, *9*, 3131−3143.
(17) Grover, W. H.; Ivester, R. H. C.; Jensen, E. C.; Mathies, R. A. *Lab Chip* **2006**, *6*, 623−631.
(18) Takao, H.; Ishida, M.; Sawada, K. *J. Microelectromech. Syst.* **2002**, *11*, 421−426.
(19) Unger, M. A.; Chou, H. P.; Thorsen, T.; Scherer, A.; Quake, S. R. *Science* **2000**, *288*, 113−116.
(20) Lai, H.; Folch, A. *Lab Chip* **2011**, *11*, 336−342.
(21) Thorsen, T.; Maerkl, S. J.; Quake, S. R. *Science* **2002**, *298*, 580−584.
(22) Tay, S.; Hughey, J. J.; Lee, T. K.; Lipniacki, T.; Quake, S. R.; Covert, M. W. *Nature* **2010**, *466*, 267−271.
(23) Jovic, A.; Howell, B.; Cote, M.; Wade, S. M.; Mehta, K.; Miyawaki, A.; Neubig, R. R.; Linderman, J. J.; Takayama, S. *PLoS Comput. Biol.* **2010**, *6*, e1001040.
(24) Jovic, A.; Wade, S. M.; Miyawaki, A.; Neubig, R. R.; Linderman, J. J.; Takayama, S. *Mol. BioSyst.* **2011**, *7*, 2238−2244.
(25) Duffy, D. C.; McDonald, J. C.; Schueller, O. J. A.; Whitesides, G. M. *Anal. Chem.* **1998**, *70*, 4974−4984.
(26) Mosadegh, B.; Tavana, H.; Lesher-Perez, S. C.; Takayama, S. *Lab Chip* **2011**, *11*, 734−742.
(27) Yaffe, D.; Saxel, O. *Differentiation* **1977**, *7*, 159−166.
(28) Kurian, N.; Hall, C. J.; Wilkinson, G. F.; Sullivan, M.; Tobin, A. B.; Willars, G. B. *J. Pharm. Exp. Ther.* **2009**, *330*, 502−512.
(29) Wlodkowic, D.; Skommer, J.; Darzynkiewicz, Z. *Cytometry, Part A* **2008**, *73A*, 496−507.